Presented at the GSI 7th Heavy Ion Collision Conference, Darmstadt, W. Germany, October 8-13, 1984; and to be published in the Proceedings

LBL--18861

DE85 007125

Pion Source Parameters in Heavy Ion Collisions

K.M. Crowe,[a] J.A. Bistirlich,[a] R.R. Bossingham,[a] H.R. Bowman,[a] C.W. Clawson,[h] K.A. Frankel,[a] O. Hashimoto,[b] T.J. Humanic,[a] J.G. Ingersoll,[a] M. Koike,[b] J.M. Kurck[a] C.J. Martoff,[a] W.J. McDonald,[c] J.P. Miller,[d] D.L. Murphy,[a] J.O. Rasmussen,[a] J.P. Sullivan,[a],[g] P. Truol,[e] E. Yoo,[a] and W.A. Zajc[a],[f]

(a) Lawrence Berkeley Laboratory, University of California, Berkeley, CA 94720
(b) Institute for Nuclear Study, University of Tokyo, Tanaski, Tokyo 1888, Japan
(c) University of Alberta, Edmonton, Alberta, Canada T6G 2J1
(d) Boston University, Boston, MA 02215
(e) University of Zurich, 8001 Zurich, Switzerland
(f) University of Pennsylvania, Philadelphia, PA 19104
(g) Texas A&M University, College Station, TX 77843
(h) Tekronix, 50-324, P.O. Box 500, Beaverton, OR 97077

Following the early work of Goldhaber, Goldhaber, Lee, and Pais[1], many experiments have used the momentum correlations between identical bosons to determine the space-time extent of the pion source for various reactions between elementary hadrons. This technique, known as intensity interferometry, has recently been applied to nuclear collisions at both intermediate[2,3,4] and very high energies[5]. Here we report on measurements of the radius and lifetime of the pion source in the reactions 1.8 A Gev ^{40}Ar+KCl → $2\pi^{\pm}$ + X, 1.8 A Gev ^{20}Na+NaF → $2\pi^{-}$ + X, and 1.71 A Gev ^{56}Fe + Fe → $2\pi^{-}$ + X.

In principle, intensity interferometry can provide a detailed picture of the size, shape, and lifetime of the pion source, as well as determining the extent to which the pion emission process is a coherent one[6]. In practice, the complications due to finite statistics, final-state interactions and other abmiguities in the analysis procedure make precision measurements very difficult. A discussion of these effects in the context of the present analysis may be found elsewhere[7].

This paper concentrates on the results most relevant to space-time models of the pion source in relativistic nuclear collisions. Assume that the pion source distribution is well-approximated by the form

$$\rho(r,t) = \frac{1}{\pi^2 R^3 \tau} e^{-\frac{r^2}{R^2} - \frac{t^2}{\tau^2}} \qquad (1)$$

In the above equation, the Gaussian distribution of the time variable reflects the expectation that the pion production process will consist of several independent emissions (thereby forming a statistical ensemble),

rather than the decay of a single excited state (which would lead to an exponential dependence). The fundamental result of intensity interferometry[6] states that the correlation function $C_2(q,q_o)$, defined as the ratio of the two-particle inclusive probability to the product of the single-particle probabilities, is given by

$$C_2(q,q_o) = 1 + |\tilde{\rho}(q,q_o)|^2 \qquad (2)$$

where $\tilde{\rho}(q,q_o)$ is the Fourier transform of $\rho(r,t)$ with respect to q and q_o, and q,q_o are, respectively, the magnitudes of the momentum difference and the energy difference of the two pions. Therefore, calculation of $C_2(q,q_o)$ from an appropriate set of two-pion events permits determination of both R and τ. Note that the normalization of $\rho(r,t)$ implies that $C_2(q=0,q_o=0) = 2$. This result depends essentially on the assumption of statistically independent emission of the pions[6] (more precisely, the pion field should be a maximally chaotic ensemble). While deviations of the intercept of C_2 from the value of 2 are often cited as evidence for a coherent component in the pion source, the possibility of such trivial effects as final state interactions or pion production via the decay of long-lived resonances should be kept in mind.

This experiment used the Berkeley Bevalac to produce beams of 1.8 A Gev ^{40}Ar, incident on a KCl target; 1.8 A GeV ^{20}Ne incident on a NaF target; or 1.71 A GeV ^{56}Fe incident on stainless steel and natural Fe targets. Any of the cases provides a near-symmetric projectile-target combination. Target thicknesses of 0.5 to 1.0 g/cm^2 provided a good compromise between the demands of high counting rate and high momentum resolution. Pions produced at $(45 \pm 8)^o$ in the laboratory were accepted into a broad-band magnetic spectrometer (Fig. 1). For the Fe+Fe measurements, an additional dipole magnet was placed at the target position so that pions produced near 0^o could be studied. Four MWPC's with 2mm wire spacing determine the momentum of accepted pions to better than 2% for $|\vec{p}_{lab}| > 200$ MeV/c.

A scintillator hodoscope is used to provide a two-pion trigger for each event. The geomtric overlap of the 'A' counters with 'B' counters defined a set of 17 possible AB combinations. A good two-pion trigger was defined as the presence of any two (different) AB combinations in conjunction with signals from the S-counters and the MWPC's. The S-counters also served to define t=0 for the time-of-flight measurements. The time-of-flight and pulse-height in each of these counters are recorded to allow for off-line proton rejection. In the case of the ^{40}Ar+KCl system both $2\pi^-$ and $2\pi^+$ data were taken, while for the ^{20}Ne+NaF and ^{56}Fe+Fe only $2\pi^-$ triggers were used. On the order of 10^4 two-pion pairs were analyzed for each of these pion polarities and target-projectile combinations.

Off-line analysis begins by using geometric criteria to identify good track candidates. These candidates are further selected by parametrizing each particle's vector momentum and initial target location in terms of MWPC hit coordinates. This parametrization is obtained by fitting Monte Carlo generated data to a Chebyshev expansion. The intrinsic precision of this procedure is very high, so that the final momentum resolution is completely determined (for low energy pions) by multiple scattering in the

target, air, and detectors; or (for high energy pions) by the finite spatial resolution of the MWPC's.

Events containing a pair of accepted pions are used to generate the correlation function. Each pion in a good pair event is required to have 220 MeV/c < $|\vec{p}_{lab}|$ < 800 MeV/c, which provides a sample of events with high momentum resolution and very low proton contamination (<2%). The correlation function is created from these events by dividing the number of actual pairs in a q and q_o bin, $A(q,q_o)$, by the number of background pairs in the same bin $B(q,q_o)$. The background events are generated by combining individual pions taken from different good two-pion events.

Intuitively, it would appear that this procedure for creating the background removes all correlations between particles within an event, while accurately reflecting the effects of the spectrometer acceptance. However, it is straightforward to demonstrate that a residual influence of the correlations found in the real events persists in the $B(q,q_o)$ generated by mixing pions from different events.[7] Extraction of the correlation function from the ratio of A to B therefore involves an iterative procedure. Also included in this iteration procedure is the effect of the Coulomb repulsion between the two like pions. Since this repulsion is maximal for those events where $q = q_o$, and since many of our events have $q \approx q_o$, it is essential that this effect, which tends to reduce the number of pairs with small relative momentum, be included in the analysis procedure. A detailed account of the Coulomb corrections and the iteration method may be found in Ref. 7.

Typical (Gamow-corrected) results are presented in Fig. 2 for Ne+NaF and Ar+KCl. Shown there are projected correlation functions $\langle C_2(q)\rangle$ and $\langle C_2(q_o)\rangle$ defined by

$$\langle C_2(q)\rangle = \frac{\sum_{q_o} A(q,q_o)}{\sum_{q_o} B(q,q_o)}, \qquad \langle C_2(q_o)\rangle = \frac{\sum_{q} A(q,q_o)}{\sum_{q} B(q,q_o)} \tag{3}$$

while these projections are no longer true correlation functions, they are indeed adequate to demonstrate the range of the data and the quality of the subsequent fits. Also shown in Fig. 2 are the results of fitting the (unprojected) correlation functions to the form

$$\alpha\left(1 + \lambda e^{-\frac{1}{2}q^2R^2 - \frac{1}{2}q_o^2\tau^2}\right) \tag{4}$$

which, aside from the parameter λ, is the C_2 corresponding to the source density given by Eq. 1. The parameters α is used to renormalize the C_2's presented in Fig. 2 so that their asymptotic value is one. The parameter

λ, which would be unity for a perfectly chaotic (i.e., incoherent) pion source, is left free to avoid introducing systematic errors in the determination of R and τ due to possible effects of coherence, final state interactions, event contamination, etc.

The results of fitting to Eq. 4 via a Principle of Maximum Likelihood procedure are given in Table 1. The errors quoted in all cases are statistical only. The values obtained for λ are substantially less than unity, and are thus consistent with a sizeable (50%) coherent component in the pion source. However, the iterative procedure used to calculate the correlation functions introduces systematic errors in the determination of λ that prohibit any strong statement concerning the significance of this result. The measurement of R and τ are much less subject to these difficulties, so that the statistical error is the dominant error in determing these quantities.

The other measurements[10] of the pion source parameters for Ar+KCl were $2\pi^-$ streamer chamber results which found at 1.2 A GeV:

$$\lambda = 0.74 \pm 0.17, \quad R = 3.8 \pm 0.5 \text{ fm}, \quad c\tau = 5.4 \pm 1.8 \text{ fm}$$

and, at 1.5 A Gev:

$$\lambda = 1.2 \pm 0.2, \quad R = 4.7 \pm 0.5 \text{ fm}, \quad c\tau = 4.2^{+1.8}_{-4.2} \text{ fm}.$$

In analyzing the Fe+Fe data, we assumed the pion source was axially symmetric, such that Eq. 1 is now expresed in terms of the parameters $R_\perp$, $R_\parallel$, and τ, the radius parameters transverse and longitudinal to the beam direction, and the lifetime parameter, respectively. This changes the functional dependence in Eqs. 2-4 such that $(q,q_0) \rightarrow (q_\parallel, q_\perp, q_0)$; otherwise the analysis methods are the same as described above.

Figure 3 shows the experimental results for Fe+Fe, along with predictions for the pion source parameters obtained from Ref. 11 using Cugnon's CASCADE code. An oblate source ($R_\perp > R_\parallel$) is measured for both pion momentum cuts at 45° ($k_1, k_2 > k_{MIN}$) and for the 0° geometry, and CASCADE is seen to agree with these results. Within the context of CASCADE, oblate shapes can be shown to result from the shadowing of pions by nuclear matter present in the collision.[11] CASCADE is seen to not describe the experimental λ parameters for k_{MIN} = 100 MeV/c.

This work was supported by the Director, Office of Energy Research, Division of Nuclear Physics at the Office of High Energy and Nuclear Physics of the U.S. Department of Energy under Contract DE-AC03-76-SF00098. Further support was provided by the INS-LBL collaboration program, Institute for Nuclear Study, University of Tokyo, JAPAN.

Table 1. Pion source parameters for Gamow corrected data.

	R(fm)	cτ(fm)	λ	χ^2/NDF
Ar + KCl → $2\pi^-$ + X	$2.88^{+0.5}_{-0.9}$	$3.29^{+1.4}_{-1.6}$	0.63 ± 0.04	98.2/80
Ar + KCl → $2\pi^+$ + X	$4.20^{+0.4}_{-0.6}$	$1.54^{+2.4}_{-1.54}$	0.73 ± 0.07	67.1/81
Ne + NaF → $2\pi^-$ + X	$1.83^{+0.8}_{-1.6}$	$2.96^{+0.9}_{-1.0}$	0.59 ± 0.08	125.7/82

REFERENCES

1. G. Goldhaber, S. Goldhaber, W. Lee, and A. Pais, Phys. Rev. 120, 300 (1960).
2. S.Y. Fung et al., Phys. Rev. Lett. 41, 1592 (1978).
3. J.J. Lu et al., Phys. Rev. Lett. 46, 898 (1981).
4. D. Beavis et al., Phys. Rev. C27, 910 (1983).
5. T. Akesson et al., Phys. Lett. 219B, 263 (1983).
6. M. Gyulassy, S.K. Kaufmann, and L. Wilson, Phys. Rev. C20, 2267 (1979).
7. W.A. Zajc et al., Phys. Rev. C29, 2173 (1984).
8. J. Cugnon and S.E. Koonin, Nucl. Phys. A335, 477 (1981).
9. J. Cugnon and D. L'Hote, Nucl. Phys. A397, 519 (1983).
10. D. Beavis et al., Phys. Rev. C29, 2561 (1983).
11. T.J. Humanic, LBL-18817, submitted to Phys. Rev. C.

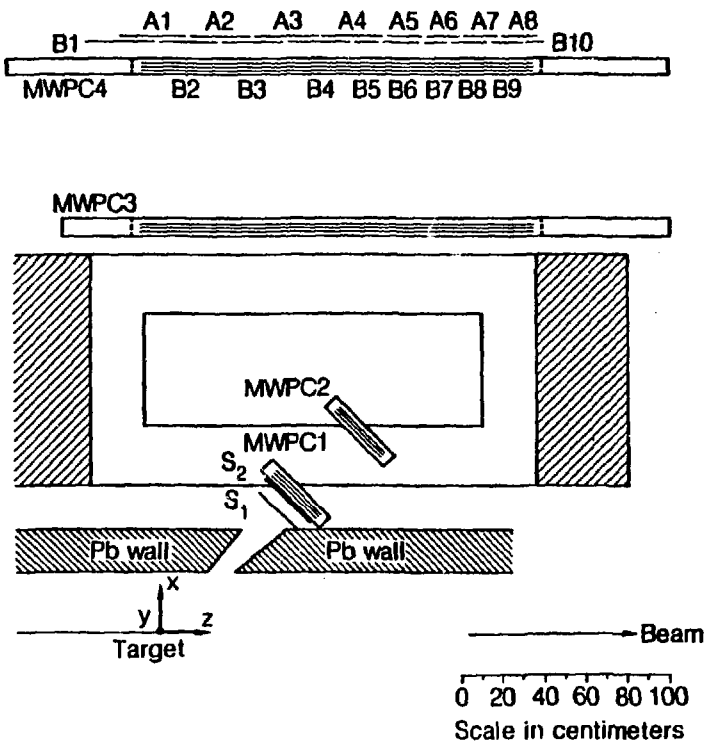

Figure 1

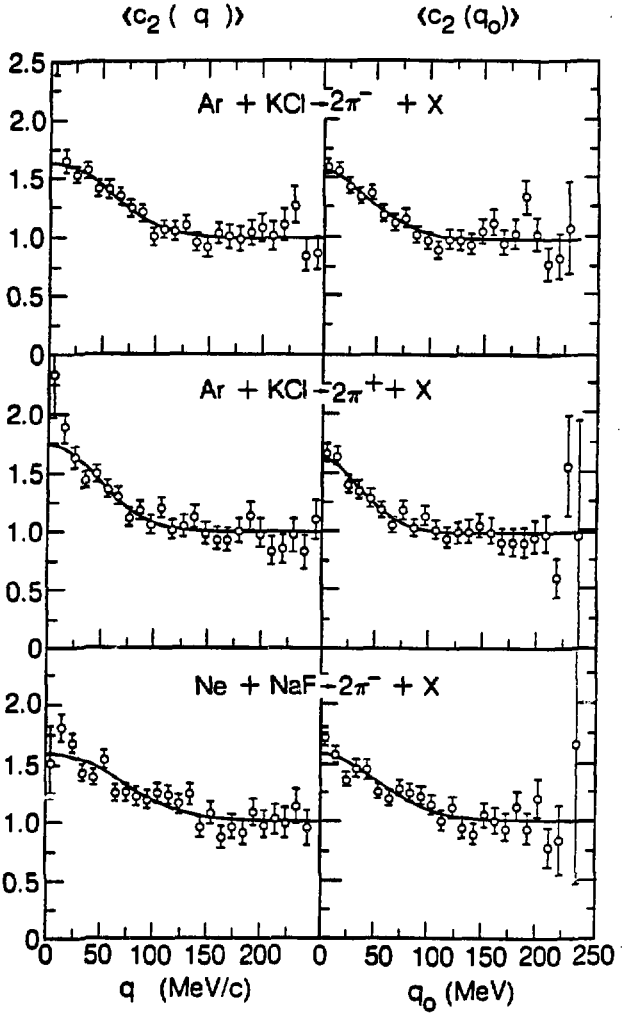
⟨c2 (q)⟩
⟨c2 (q0)⟩
Ar + KCl → 2π⁻ + X
Ar + KCl → 2π⁺ + X
Ne + NaF → 2π⁻ + X
2.5
2.0
1.5
1.0
0.5
0
0 50 100 150 200
q (MeV/c)
0 50 100 150 200 250
q0 (MeV)

Figure 2

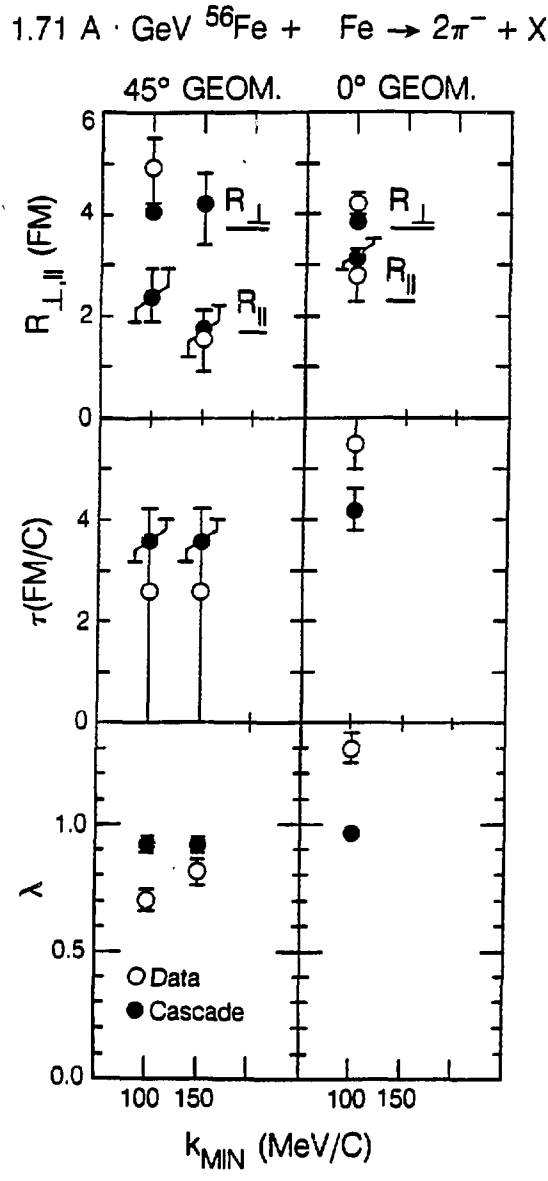

Figure 3

XBL 8411-8935